Astrophysical explanations of PAMELA/ATIC

Alexander Kartavtsev

16:00–17:30, Thursday, 7 May 2009

1 The standard scenario

1.1 General information

- Astrophysical observations indicate, that the amount of antimatter in the Universe is very small. Most of the observed antimatter is created in the collision of the cosmic rays (CR) with interstellar medium (ISM). To calculate the positron fraction we need to know properties of the interstellar medium and of the cosmic rays.
- The studies of the atmospheric showers allow us to measure the composition and energy spectrum of the cosmic rays. Roughly speaking, almost 90% of all the incoming cosmic rays are protons, about 9% are helium nuclei and about 1% are electrons. The energy spectrum is described by a power law: **flux** $\propto E^{-\gamma}$. Below the "knee" the spectral index is equal to $\gamma \approx 2.7$, above the "knee" $\gamma \approx 3.1$.
- The interstellar medium consists of an extremely dilute mixture of ions, atoms, molecules, larger dust grains, cosmic rays, and galactic magnetic fields. As the cosmic rays propagate, they interact with the protons and helium atoms of the interstellar medium and produce, among other species, pions and kaons.

Thus according to the standard scenario the only source of positrons in the cosmic rays are the collisions of the cosmic ray particles with interstellar medium.

1.2 Production of secondary positrons

- There many sources of positrons in the Galaxy [1]:
  - **secondaries in the $\pi^+ \to \mu^+ \to e^+$ chain (and from various kaon decay modes);**
  - **positrons produced in individual sources;**
  - produced by interactions of cosmic ray nuclei with the ISM;
  - decay products of excited nuclei of both the ISM and cosmic rays;
  - e^+e^- pairs from γ–ray interactions in the ISM.

The first two sources give the largest contributions.

- The pions are produced in the proton–proton and proton–helium interactions of the cosmic rays with the interstellar medium. The resulting pion energy distribution is to a first approximation also a power law with the same slope.

- Pions decay mostly into muons and muon (anti)neutrinos: $\pi^+ \rightarrow \mu^+ + \nu_\mu$ **and** $\pi^- \rightarrow \mu^- + \bar{\nu}_\mu$. Muons in turn decay mostly into an electron or positron, electron (anti)neutrino and muon (anti)neutrino: $\mu^+ \rightarrow e^+ + \nu_e + \bar{\nu}_\mu$ **and** $\mu^- \rightarrow e^- + \bar{\nu}_e + \nu_\mu$.

- Just like pions, kaons predominantly decay into muon and muon (anti) neutrino: $K^+ \rightarrow \mu^+ + \nu_\mu$ **and** $K^- \rightarrow \mu^- + \bar{\nu}_\mu$. They also possess an important hadronic decay mode: $K^\pm \rightarrow \pi^\pm + \pi^0$. The total contribution of the kaons is not very large, at the level of a few percent.

- If the pion (kaon) spectrum has a power law form, then the resulting positron energy distribution will have the same slope.

Using information about flux and energy spectrum of protons in the cosmic rays we can calculate flux and energy spectrum of the secondary positrons.

1.3 Propagation

- High energy electrons are subject to a number of energy loss processes. The loss mechanisms involve interactions with matter, magnetic fields and radiation:

  ionization loses: in the process of ionization, electrons are torn off atoms by the electrostatic forces between the charged particles of the cosmic rays and the particles of the interstellar medium;

  bremsstrahlung: bremsstrahlung is the radiation associated with the acceleration of electrons in the electrostatic fields of ions and of the nuclei in atoms.

  adiabatic loses: the energy loss due to the expansion of the volume within which the particles are contained – the relativistic gas does the work;

  synchrotron radiation: is the radiation emitted by high energy charged particles and caused by gyrating in a magnetic field;

  inverse Compton scattering: process of scattering of electrons off photons in which the electrons loose part of their energy.

- There are also several processes which determine propagation of the produced postirons:

  diffusion: diffusion of cosmic rays results from particle scattering on random magnetohydrodynamics waves and discontinuities;

  advection: In fluids advection means that matter or heat is transported by the larger-scale motion of currents in the fluid. In astrophysics advection is caused by the galactic winds which transport the cosmic rays.

  reacceleration: In addition to spatial diffusion, the scattering of cosmic ray particles on randomly moving magnetic waves leads to stochastic acceleration.

galactic structure: Almost all aspects of galactic structure affect cosmic ray propagation, but the most important for electron energy losses are the gas content for secondary production, interstellar radiation field and magnetic field.

- Let us derive the transport equation for the cosmic rays taking into account only diffusion in its simplest form. The number of particles in the distance increment x and energy increment dE is $N(E,x,t)dEdx$. Therefore the rate of change of particle density in this little box is

$$\frac{d}{dt}N(E,x,t)\,dEdx = [\phi_x(E,x,t) - \phi_x(E,x+dx,t)]dE + [\phi_E(E,x,t) - \phi_E(E+dE,x,t)]dx + Q\,dEdx$$

where ϕ_x and ϕ_E are the fluxes of particles in the coordinate and momentum spaces respectively. Performing the Taylor expansion we find

$$\frac{dN}{dt} = -\frac{\partial\phi_x}{\partial x} - \frac{\partial\phi_E}{\partial E} + Q$$

Introducing the diffusion coefficient D, which is assumed to be constant in space and time, we can represent the flux in the coordinate space in the form:

$$\phi_x = -D\frac{\partial N}{\partial x}\,.$$

From physical considerations it is clear that the flux in the momentum space can be expressed in the form:

$$\phi_e = N(E)\frac{dE}{dt}$$

The electrons within the small volume are subject to energy gains and losses:

$$\frac{dE}{dt} = -b(E)\,.$$

Therefore, collecting all the terms we obtain

$$\frac{dN}{dt} = -D\nabla^2 N + \frac{\partial}{\partial E}[b(E)N(E)] + Q(E)$$

- Next we consider solution of this equation. We assume a uniform distribution of sources each injecting electrons with an injection spectrum of the form $Q = \kappa E^{-\ell}$. Due to the uniform distribution the diffusion term is not important and we can easily solve the transport equation. Given the boundary condition $N(E) \to 0$ as $E \to \infty$ we obtain the following stationary solution:

$$N(E) = \frac{\kappa E^{-(\ell-1)}}{(\ell-1)b(E)}$$

For high–energy electrons and positrons the energy loses are dominated by the inverse Compton scattering and synchrotron emission. In both cases $b \propto E^2$, so that $N(E) \propto E^{-(\ell+1)}$. That is, the spectrum is steeper by one power of E.

- The electrons are accelerated by the same astrophysical sources as the protons. It is usually assumed, that the injection spectrum of electrons in astrophysical sources, such as supernova remnants, is the same as the injection spectrum of protons, i.e. $\ell = p$. Therefore energy spectrum of the electrons observed on the Earth is $N_{e^-}(E) \propto E^{-(p+1)}$.
- Proton lose part of their energy due to all of the above mechanisms. In addition they loose energy in the collisions with interstellar matter particles producing heavier elements. Empirically proton spectrum as observed on the Earth is $N_p(E) \propto E^{-(p+\delta)}$. Analysis of boron to carbon ratio allows us to determine $\delta = 0.3 \ldots 0.6$.
- Since injection spectrum of the secondary positrons coincides with spectrum of the protons and positrons loose energy in the same way as electrons, we have $N_{e^+}(E) \propto E^{-(p+\delta+1)}$.
- Injection spectra and spectra observed near the Earth are summarized in the table bellow:

particle	**injected**	**observed**
protons	p	p+δ
electrons	p	p+**1**
positrons	p+δ	p+δ+**1**

- For the positron fraction we then obtain in the first approximation

$$\frac{e^+}{e^+ + e^-} \sim E^{-\delta}$$

- The results of numerical computation are presented in Fig. 1.

In the standard scenario we expect the positron fraction to decrease with energy, whereas the observations tell us that above 10 GeV it increases with energy. [2, 3].

2 Astrophysical solutions

- A possible solution to this problem is the existence of some additional primary sources of positrons.
- Let us assume that:
  - in the standard scenario flux of primary electrons is P_{std}
  - flux of secondary electrons and positrons is S
  - then the positron fraction is
$$f = \frac{S}{P + 2S}$$
  - if furthermore there are other primary sources of electrons and positrons, P_{new} ,then the positron fraction reads
$$f = \frac{S + P_{new}}{P + 2S + 2P_{new}}$$
  - if the new sources are stronger than the conventional ones, then the positron fraction increases.

2.1 The pulsar explanation

- One of the most popular explanations attributes the excess of electrons to the nearby pulsars.
- Although a self-consistent quantitative description of pulsar electrodynamics is yet to be formulated, energy considerations and observed emission properties (e.g. at radio and gamma-ray frequencies) suggest that pulsars host electron–positron pair–production processes. Therefore the PAMELA results can be explained by one single nearby pulsar or a superposition of many pulsars (1789 are known).
- As I have already mentioned, energetic electrons and positrons loose energy via the inverse Compton scattering and synchrotron emission. The lifetime of relativistic electrons and positrons against the energy losses leads to a cutoff in the energy

  $$E^{max} \sim 3 \left(\frac{10^5 \mathrm{yr}}{t} \right) \mathrm{TeV}$$

  This implies that electrons with energies not exceeding 1 TeV must have been injected not longer than **10^5 years** ago. Using typical values of the diffusion coefficient D we can furthermore estimate the distance they must have originated from: $\sqrt{D \times t} \sim 100 - 500$ pc [4]. So we must look for the sources of the positron excess in this region. The existing catalogues of pulsars contain objects precisely in this range.
- A few words about pulsars are in place here.
  - According to the current understanding of the problem, a pulsars is neutron star, whose magnetic field is not aligned with its spin axis. This model is often referred to as an "oblique rotator" [5].
  - Due to the fact that the magnetic dipole is oriented at an angle with respect to the rotation axis, there is a varying dipole moment at a large distance. This results in the radiation of electromagnetic energy from the dipole, which is extracted from rotational energy of the neutron star. This breaking mechanism implies that

    $$\dot{\Omega} = -K\Omega^n, \quad n = 3$$

    This formula allows us to estimate age of the pulsar, $\tau \approx -\Omega/2\dot{\Omega}$, Ω being the angular frequency of rotation. A typical lifetime for the majority of pulsars is 10^7 **years**, i.e. in the right ballpark.
  - Outside the neutron star the Lorentz force far exceeds the force of gravity – the ratio of the two is $\sim e\Omega r^3 B/GMm_e \sim 10^{12}$ for the case of the Crab pulsar. Furthermore, the induced electric field at the surface exceeds the work function of the surface material, and consequently there must be a plasma surrounding the neutron star. The plasma is entirely **charge–separated**.
  - The charge density in the pulsar magnetosphere is high enough to screen the electric field parallel to the pulsar magnetic field, hence the co–rotation condition $E \cdot B = 0$ is maintained everywhere except in a few locations. These regions, where $E_{||} \neq 0$, are located: (1) close to the surface of the neutron star in the polar caps (polar cap or inner gaps models) and (2) at distances comparable with the light cylinder of the pulsar along the null charge surface defined by the condition $\Omega \cdot B = 0$, where the co–rotation charge density changes sign (outer gap models) [4].

– In both scenarios ultra–relativistic electrons are restricted to move along the super-strong magnetic field at the neutron star surface, and synchrotron–radiate very energetic curvature photons at high energy gamma–ray frequencies. In turn, such curvature photons cannot escape from the pulsar, since the magnetic field in the vicinity of the stellar surface is so strong that they are efficiently converted into $e^{\pm}$ pairs by it. Most $e^{\pm}$ pairs are actually created beyond the polar caps, and are moving toward the pulsar light cylinder eventually escaping from the cylinder instead of being annihilated at the stellar surface. Beyond the light cylinder, they add up to the pulsar wind and finally flow out, further accelerated by low-frequency electromagnetic waves in the nebula.

- Let us now estimate the energy emitted in the form of $e^{\pm}$ pairs. The simples and, of course, the most crude way to estimate it is to assume that a fraction $f_e \sim 3\%$ of the total initial pulsar energy was emitted in the form of pairs. For a pulsar with a constant momentum of inertia I the energy is given by $E = \frac{1}{2} I \Omega_0^2$. This number can be roughly estimated using the observations and typical lifetime of a pulsar:

$$E = f_e \dot{E} \frac{T^2}{\tau_0}$$

  where τ_0 is a characteristic "decay time" which cannot be directly derived from pulsar timing measurements. It is usually assumed to be of the order of 10^4 **years**.

- This crude estimate corresponds to the model in which all the $e^{\pm}$ pairs are emitted simultaneously at some point and then propagate in the Universe. This is motivated by the fact, that a pulsar emits most of the pairs during the first 10^4 years. On the other hand, it takes about 10^5 the $e^{\pm}$ pairs to reach the Earth (which is comparable to the pulsar's lifetime). Therefore to a first approximation it is irrelevant that the $e^{\pm}$ pairs have been injected not instantaneously. There are also more refined treatments [6], which lead to similar results.

- The pulsar wind cannot accelerate $e^{\pm}$ pairs to arbitrarily high energies, and a **cut–off** is expected, depending on the pulsar system, in the energy range around the **TeV scale**. Below this scale one usually assumes a power law

$$\frac{dN}{dE} \propto E^{-\alpha}$$

  The spectral index ranges from **1 to 1.6 for** $E \sim 1$ **GeV** steepening to $\alpha \approx 3.2$ **at** $E \sim 10$ **TeV**.

- There are a few most promising sources of the positron excess:

- Since we now deal with point–like sources, we can not neglect the diffusion term in the propagation equation. As a result, the observed spectrum depends on the distance of the source from Earth. The diffusion coefficient is assumed to be energy dependent, $D = D_1 E^{\delta}$, where $D_1 = 3.4 \times 10^{27}$ cm^2/s and $\delta = 0.7$ for the MED scenario and $D_1 = 1.8 \times 10^{27}$ cm^2/s and $\delta = 0.55$ for the MAX scenario.

Name	Distance [kpc]	Age [yr]	$\dot{E}$ [ergs/s]	$E_{\rm out}$ [ST]	$f_{e^\pm}$
Geminga	**0.16**	3.42×10^5	3.2×10^{34}	**0.360**	**0.005**
Monogem	**0.29**	1.11×10^5	3.8×10^{34}	**0.084**	**0.015**
Vela	**0.29**	1.13×10^4	6.9×10^{36}	**0.044**	**0.020**
B0355+54	**1.10**	5.64×10^5	4.5×10^{34}	**1.366**	**0.2**
Loop I [SNR]	**0.17**	2×10^5		***0.3***	**0.006**
Cygnus Loop [SNR]	**0.44**	2×10^4		***0.03***	**0.01**

- Results of the calculation are presented in Fig. 3. The figures show that both the **nearby Geminga pulsar and the Loop I SNR**, both at distances around **160–170 pc**, and both with ages $T \sim 2 - 3 \times 10^5$ **years**, can very naturally be **the dominant positron sources** to explain the **PAMELA** data, with an output in $e^\pm$ less than a percent of the pulsar rotational energy [4, 7]. The resulting contribution to the total $e^\pm$ at larger energies is subdominant. Young, powerful and relatively **nearby sources like Vela and the Cygnus Loop likely contribute to the highest energy part** of the total $e^\pm$ differential spectrum.

- The **Monogem** pulsar might plausibly contribute to the **higher energy bins** reported by **PAMELA**, and could be dominating the $e^\pm$ flux **between 1 and 3 TeV**, even with a $e^\pm$ efficiency factor of $f_e \simeq 1.5\%$.

- For ATIC the candidate pulsar should be distant enough for the resulting spectrum to be peaked enough around E_{bump} to avoid excessive contributions at lower energies, and bright enough to produce the right level of $e^\pm$. The **ATIC** bump might be generated by **B0355+54**, although this requires a very efficient output of $e^\pm$ ($f_e \sim 20\%$). The need in such a large efficiency means that the pulsar scenario is compatible but does not favor, for natural values of parameters, the peaked spectrum reported by ATIC.

- Note that none of the sources can alone be responsible for both PAMELA and ATIC results. To explain the data we need at least two sources.

- An attempt to take into account several pulsars is presented in Fig. 5.

- Notice that a combination of pulsars also shows a prominent drop-off feature at lower energies, which could be detected with higher statistics.

- So far we have an evidence, that pulsars can geerate enough electron–positron pairs to reproduce the PAMELA and probably also ATIC results. Next we have to check that for the chosen parameters pulsars do not overproduce positrons. The results of inclusion of the pulsars not included so far are presented in Fig. 6. In general, in all scenarios, **the positron fraction starts to increase after 100 GeV** so it is unlikely that the PAMELA positrons dominantly originate from further away than 1 kpc.

- The spectral shape of the electron excess is insufficient to discriminate a dark-matter origin from more conventional astrophysical explanations [6].

- It is theoretically possible to distinguish the two scenarios using the directional information: even after the diffusive propagation of electrons and positrons from pulsars is taken

into account, at sufficiently high energies a small dipole anisotropy should be present in the direction of the dominant nearby source(s).

- It it likely, that in the decays of dark matter particles not only charged leptons are produced, but also neutrinos. Pulsars, on the other hand are unlikely to be strong sources of TeV neutrinos [8]. Therefore, the TeV neutrinos can be potentially used to distinguish the two scenarios [9].

The pulsar scenario can naturally explain the *shape* of the curves measured by PAMELA and ATIC. The *flux* of the $e^{\pm}$ pairs, however, depends on the choice of the parameters. It should be possible to distinguish this scenario from the DM one using the directional information and, possibly, neutrinos.

2.2 Production inside the standard sources

- Cosmic rays are assumed to be accelerated in the astrophysical sources, like the supernova remnants [10, 11].

- Cosmic rays accelerated at the shock produce secondary $e^{\pm}$ pairs inside the source through hadronic interactions with production and decay of charged pions, while the decay of neutral pions leads to production of gamma rays. This process occurs in the same spatial region around the shock in which cosmic rays are being accelerated. Therefore the secondary $e^{\pm}$ take part in the same acceleration process.

- Up to several tens of GeV the $\bar{p}/p$ spectrum is in agreement with conventional mechanisms. At these energies it flattens at first. At higher energies it eventually starts rising with energy. New data at high energy from PAMELA and AMS-02 should enable us to distinguish between this explanation and a pulsar related one for the positron fraction.

- Provided that this scenario is correct, it may affect the perspectives for the detection of DM via a signature in highenergy antiprotons, since it proposes a purely astrophysical mechanism to produce a high-energy "excess" of antiprotons over the secondary yield from ISM production. An "excess" in the high-energy range of $\bar{p}/p$ could not be interpreted anymore uniquely as manifestation of new physics.

This scenario "corrects" the standard one and predicts a higher flux of positrons. A subproduct is a higher flux of antiprotons at energies above 100 GeV.

3 Summary

- **The standard scenario:**
  - Positrons are secondaries produced in collisions of cosmic rays with interstellar medium;
  - The positron fraction is expected to be a decreasing function of energy.
- **The pulsar scenario:**

  - The pulsar scenario explains the observed decrease of the positron fraction by the $e^{\pm}$ pairs emmited by nearby pulsars;
  - By picking a few nearby known pulsars one can reproduce the spectral features and intensities reported by both PAMELA and ATIC;
  - To explain both PAMELA and ATIC data simultaneously at least to sources are needed. The ATIC data requires a rather unnatural choice of the model parameters;
  - The spectral shape of the electron excess is insufficient to discriminate a dark-matter origin from more conventional astrophysical explanations;
  - It is theoretically possible to distinguish the DM and pulsar scenarios using the directional information;
  - The TeV neutrinos can be as well potentially used to distinguish the two scenarios.

- **Production inside the standard sources scenario:**
  - Corrects a "mistake" in the standard scenario – the standard sources also produce and accelerate $e^{\pm}$ pairs;
  - Also predicts high flux of antiprotons at high energies, which can be used to distinguish this scenario from the others;
  - Has an important implication for dark matter searches: it is no longer possible to attribute an excess of antiprotons in the cosmic rays to decays or anihilations of dark matte particles.

References

[1] M. Giler, J. Wdowczyk and A. W. Wolfendale, *The Energy Spectrum of Cosmic Ray Positrons*, *J. Phys.* **A10** (1977) 843–859.

[2] O. Adriani *et. al.*, *A new measurement of the antiproton-to-proton flux ratio up to 100 GeV in the cosmic radiation*, *Phys. Rev. Lett.* **102** (2009) 051101 [0810.4994].

[3] F. Collaboration, *Measurement of the Cosmic Ray e+ plus e- spectrum from 20 GeV to 1 TeV with the Fermi Large Area Telescope*, 0905.0025.

[4] S. Profumo, *Dissecting Pamela (and ATIC) with Occam's Razor: existing, well-known Pulsars naturally account for the 'anomalous' Cosmic-Ray Electron and Positron Data*, 0812.4457.

[5] M. A. Ruderman and P. G. Sutherland, *Theory of pulsars: Polar caps, sparks, and coherent microwave radiation*, *Astrophys. J.* **196** (1975) 51.

[6] M. Pohl, *Cosmic-ray electron signatures of dark matter*, 0812.1174.

[7] D. Grasso *et. al.*, *On possible interpretations of the high energy electron- positron spectrum measured by the Fermi Large Area Telescope*, 0905.0636.

[8] A. Bhadra and R. K. Dey, *TeV neutrinos and gamma rays from pulsars*, 0812.1845.

[9] J. Liu, P.-f. Yin and S.-h. Zhu, *Prospects for Detecting Neutrino Signals from Annihilating/Decaying Dark Matter to Account for the PAMELA and ATIC results*, 0812.0964.

[10] P. Blasi, *The origin of the positron excess in cosmic rays*, 0903.2794.

[11] P. Blasi and P. D. Serpico, *High-energy antiprotons from old supernova remnants*, 0904.0871.

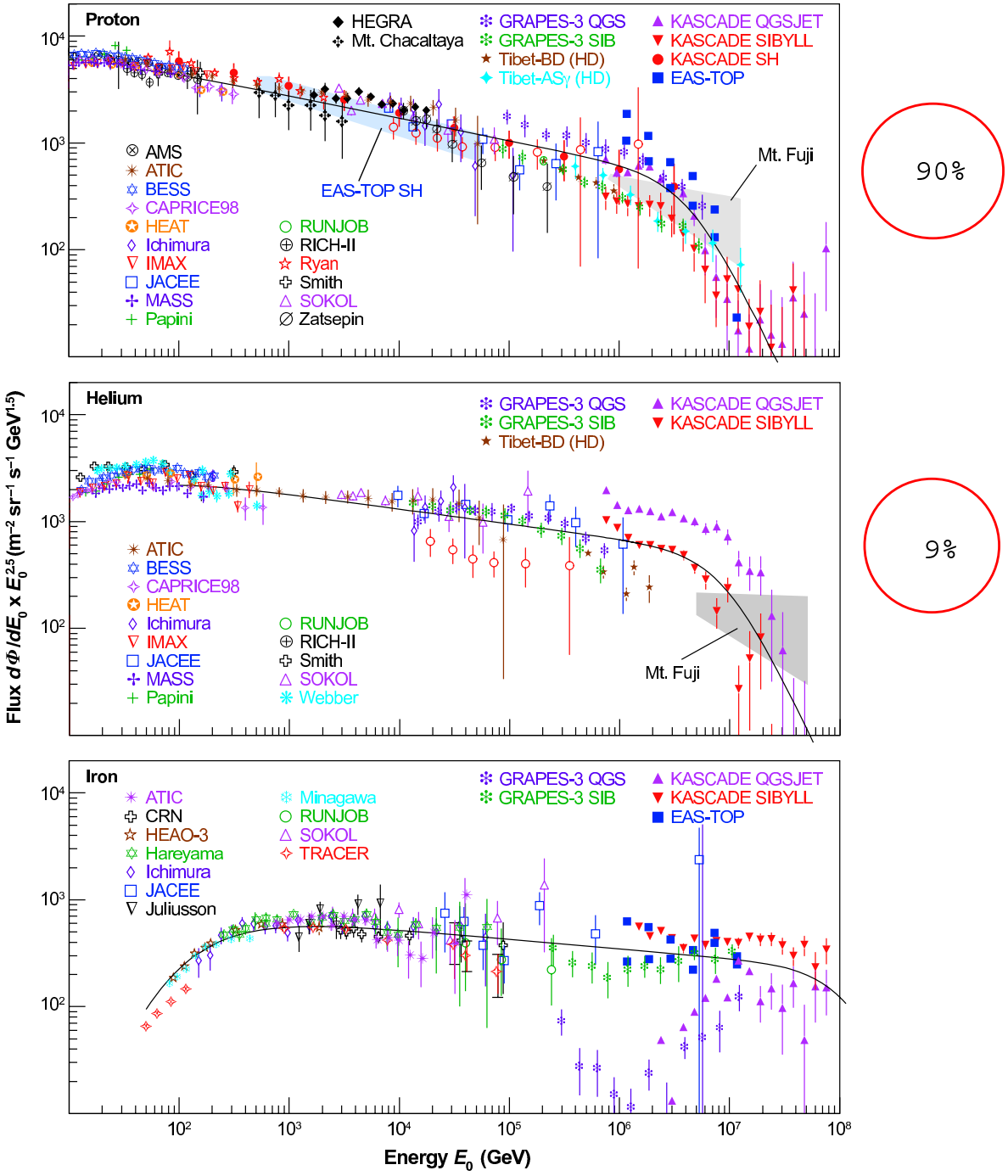

Figure 1

Compilation of spectral data 10^{10}–10^{17} eV for proton, helium, and iron, combining balloon, satellite, and ground-based measurements. Figure adapted with permission from Reference 18 and G. Hörandel (private communication).

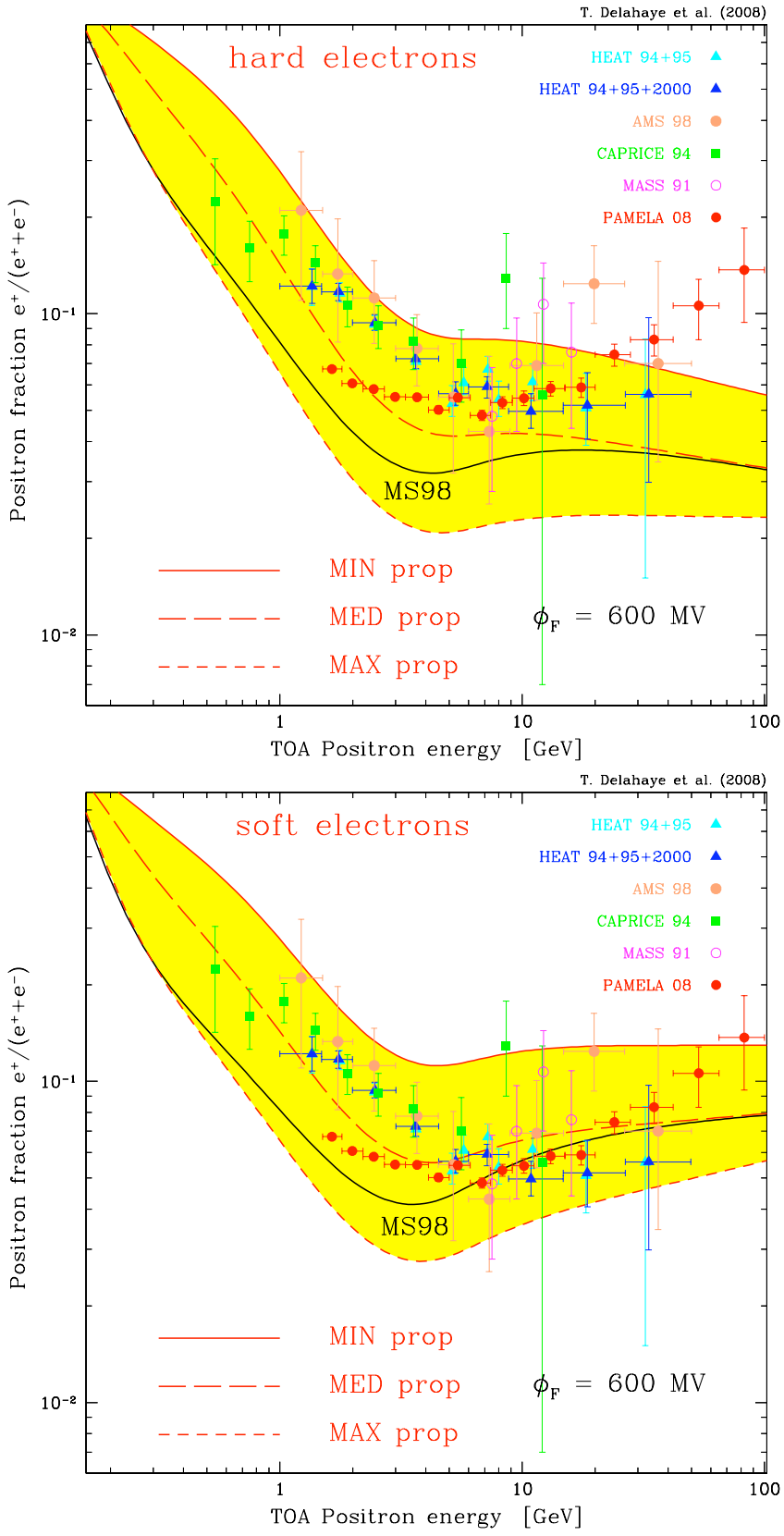

Figure 1: Positron fraction as a function of the positron energy.

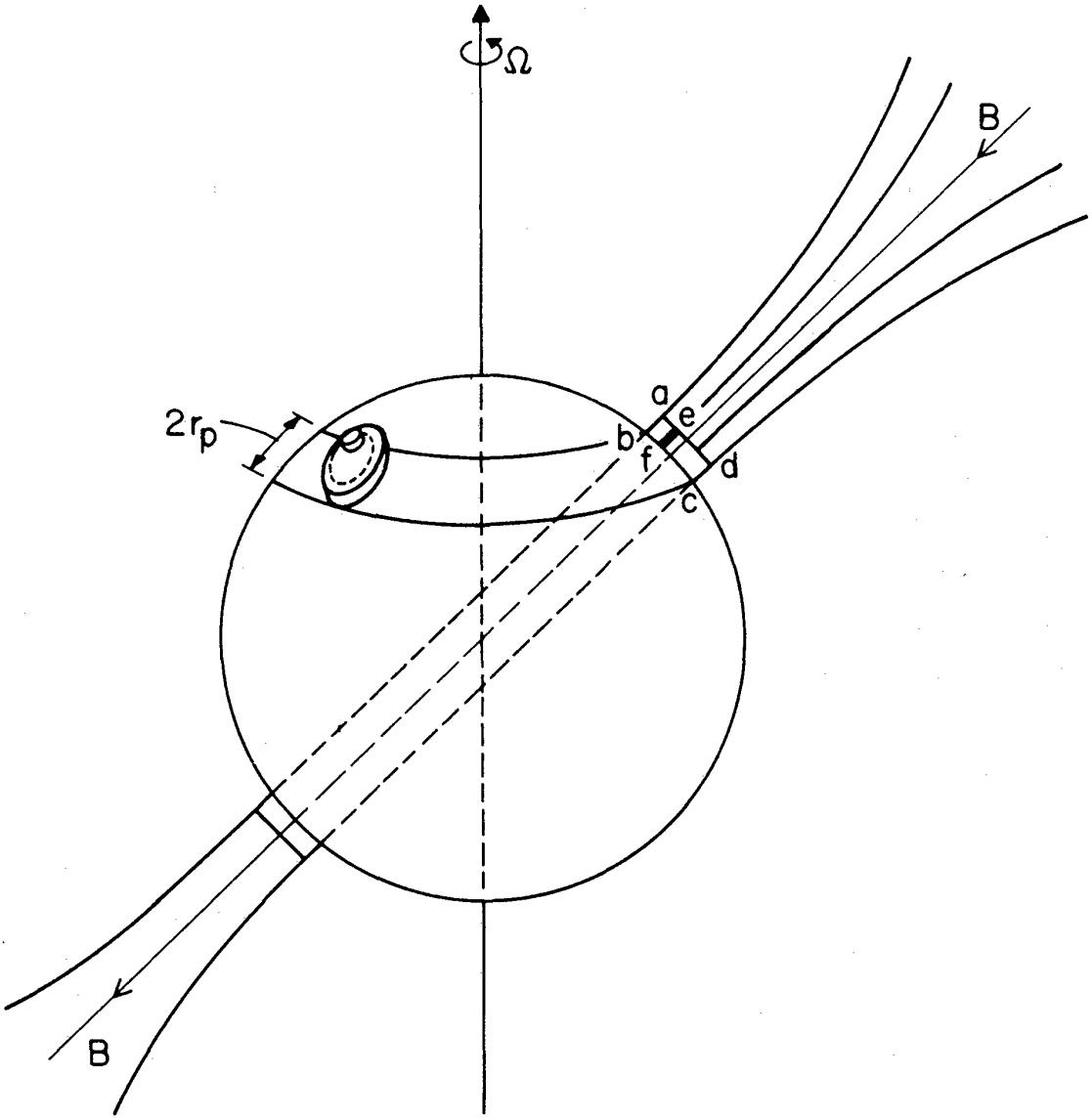

FIG. 4.—Schematic of a rotating neutron star with dipole moment somewhat inclined to the rotation axis. The polar cap, of base diameter $2r_p$, moves at fixed latitude. A spark *ef* in the gap *abcd* drifts counterclockwise on a circular path (*dashed line*) on the polar cap centered on the magnetic field axis. This spark feeds relativistic particles onto field lines: coherent microwave radiation is produced tangentially to these field lines far above ($\sim 10^8$ cm) the stellar surface.

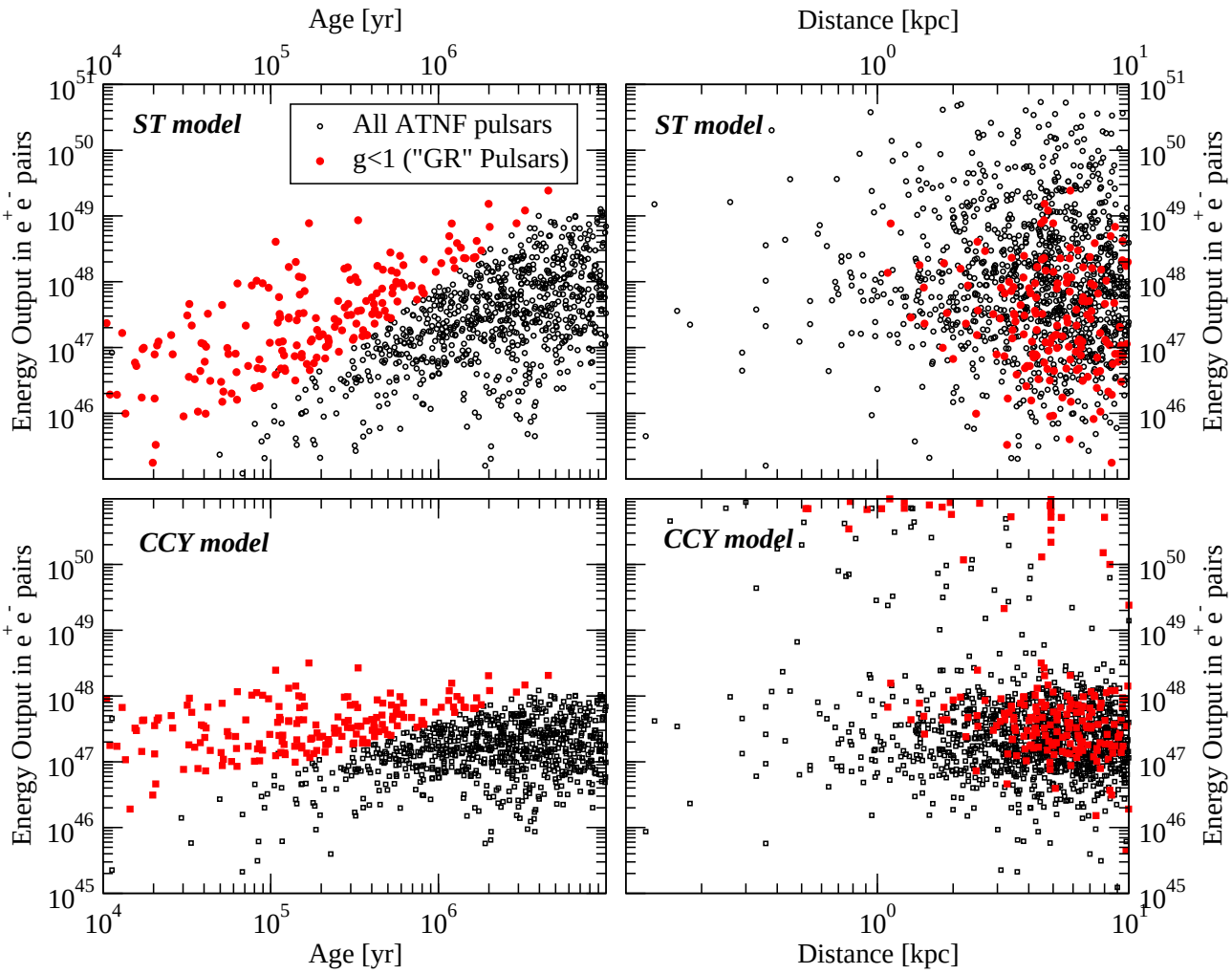

Figure 2: Scatter plot in the energy output in $e^{\pm}$ versus age (left panels) and versus distance (right panels), for the ST model and for the CCY model. The black circles indicate all pulsars in the ATNF catalogue, while the red dots indicate "gamma-ray" pulsars. From arXiv:0812.4457

Name	Distance [kpc]	Age [yr]	$\dot{E}$ [ergs/s]	$E_{\rm out}$ [ST]	$f_{e^\pm}$
Geminga	0.16	3.42×10^5	3.2×10^{34}	0.360	0.005
Monogem	0.29	1.11×10^5	3.8×10^{34}	0.084	0.015
Vela	0.29	1.13×10^4	6.9×10^{36}	0.044	0.020
B0355+54	1.10	5.64×10^5	4.5×10^{34}	1.366	0.2
Loop I [SNR]	0.17	2×10^5		*0.3*	0.006
Cygnus Loop [SNR]	0.44	2×10^4		*0.03*	0.01

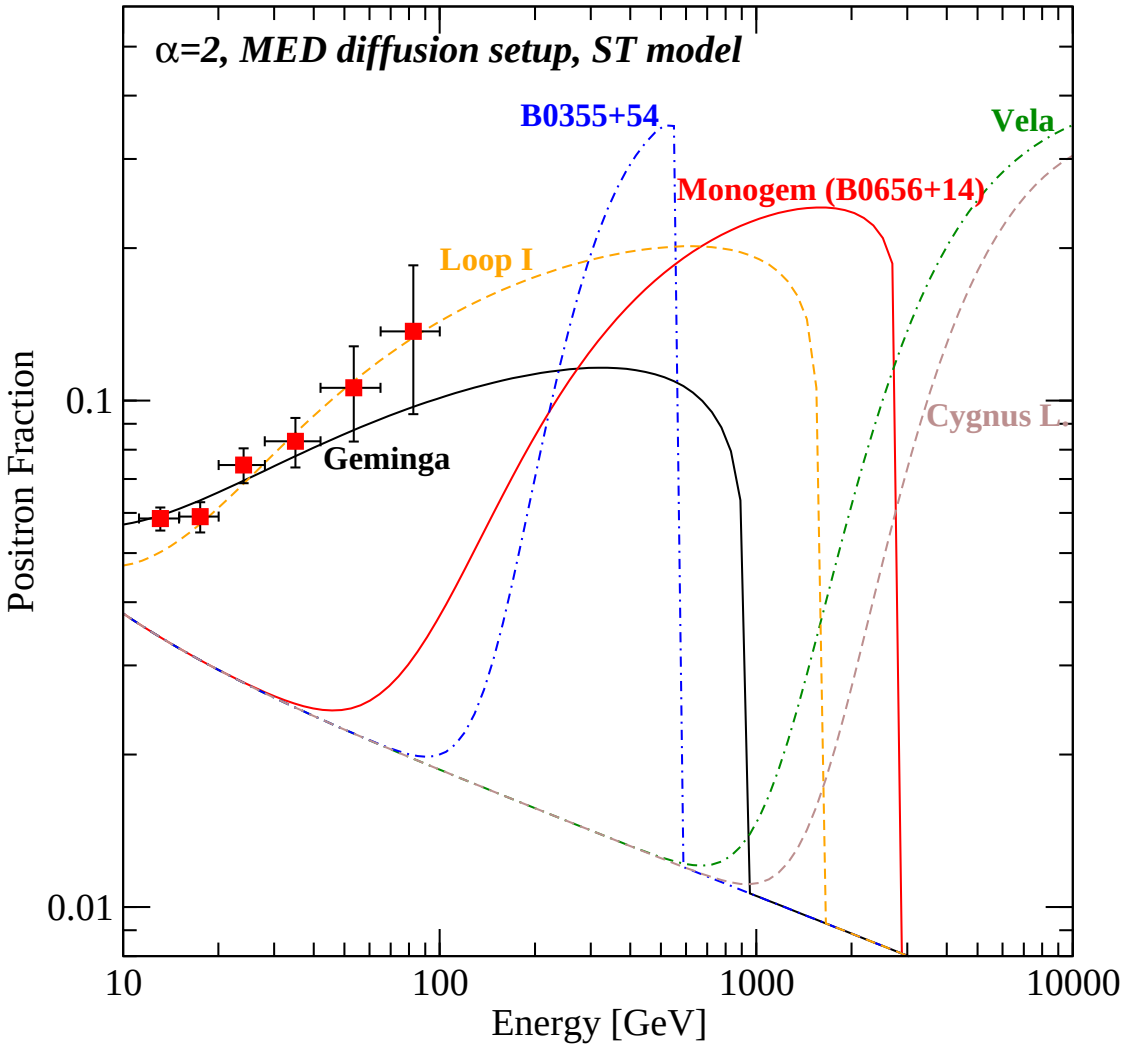

Figure 3: The positron fraction: comparison with the PAMELA data. From arXiv:0812.4457

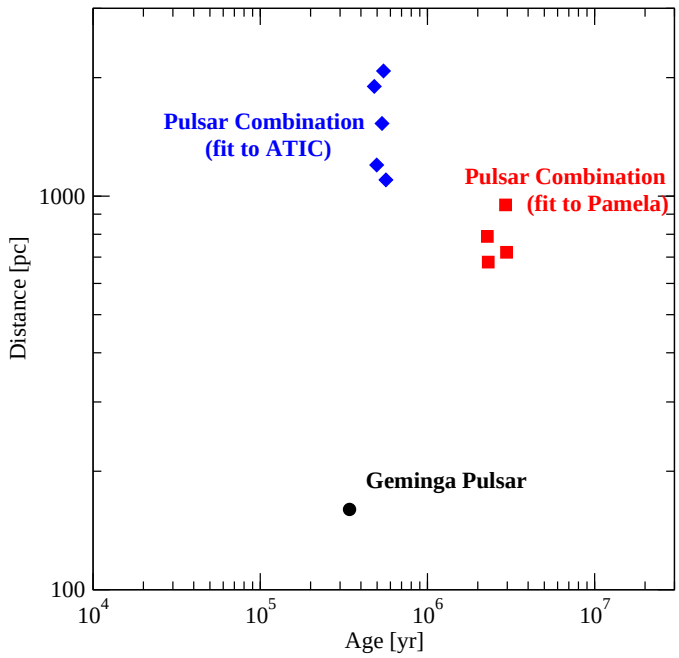

Figure 4: The location, in the age versus distance plane, of the pulsars.

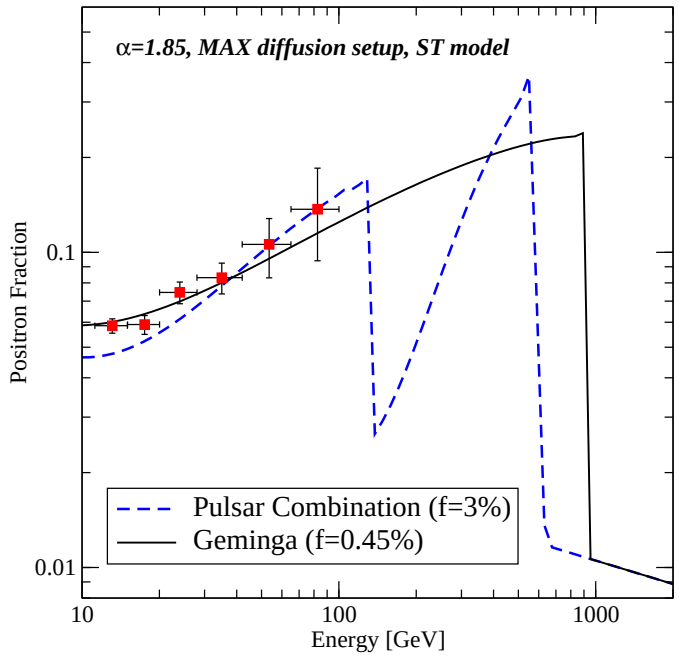

Figure 5: The positron fraction: comparison with the PAMELA data. From arXiv:0812.4457

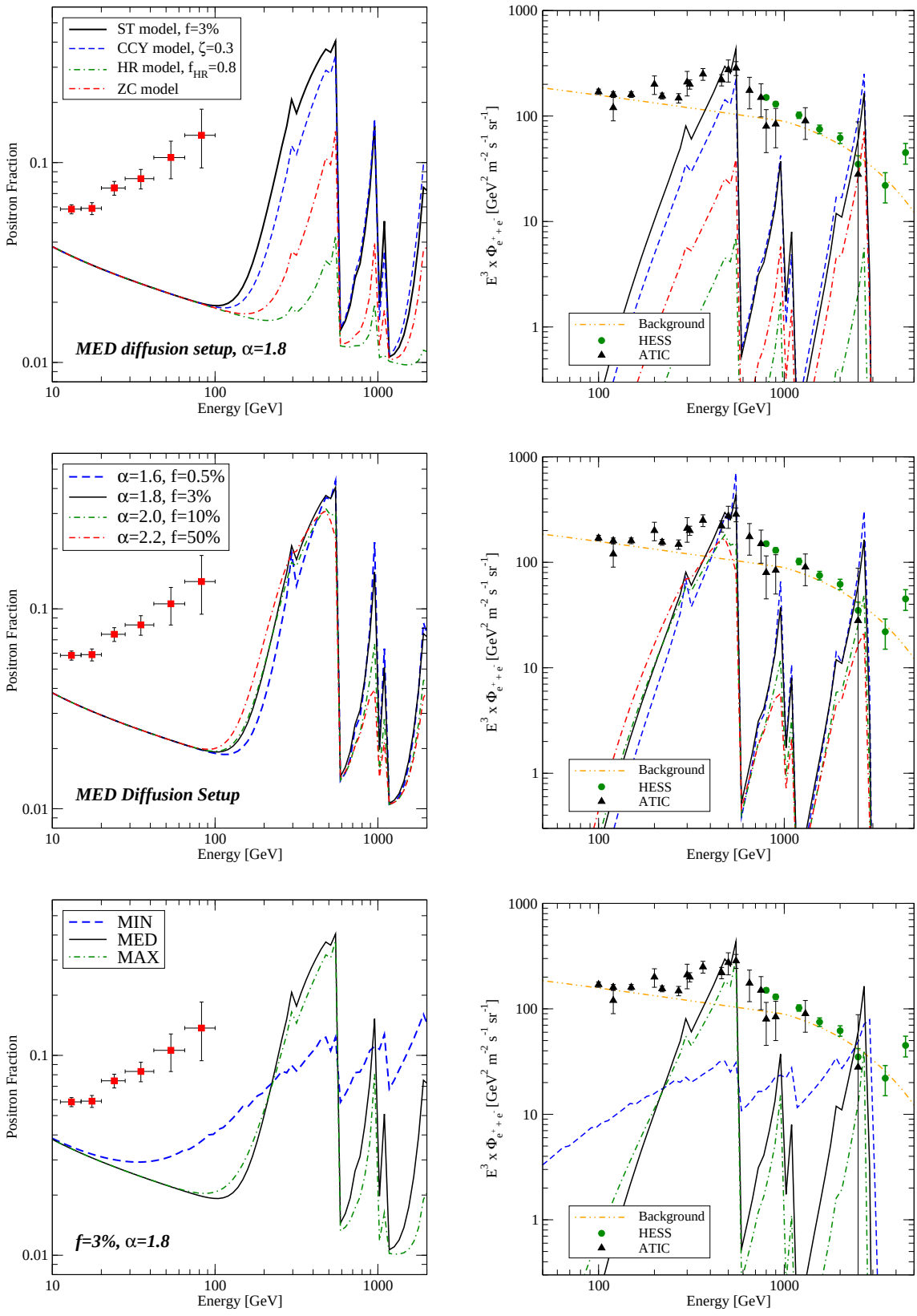

Figure 6: The contribution from all gamma-ray pulsars ($g < 1$) in the ATNF catalogue located at a distance greater or equal than 1 kpc.